# Radiative transition processes of light vector resonances in a chiral framework

Yun-Hua Chen,[1] Zhi-Hui Guo,[2,*] and Han-Qing Zheng[3]

[1]*Institute of High Energy Physics, CAS, Beijing 100049, People's Republic of China*
[2]*Department of Physics, Hebei Normal University, Shijiazhuang 050024, People's Republic of China
and State Key Laboratory of Theoretical Physics, Institute of Theoretical Physics,
Chinese Academy of Sciences, Beijing 100190, People's Republic of China*
[3]*Department of Physics and State Key Laboratory of Nuclear Physics and Technology, Peking University,
Beijing 100871, People's Republic of China*

Within the framework of chiral effective field theory, we study various electromagnetic processes with light vector resonances: $K^*(892) \to K\gamma$, $e^+e^- \to K^*(892)K$, and the $\omega\pi\gamma^*$ form factors. With two multiplets of vector resonances being introduced, we fit the decay widths of $K^{*0} \to K^0\gamma$, $K^{*+} \to K^+\gamma$, and the pertinent measurements from the $e^+e^- \to K^{*\pm}(892)K^\mp$ cross sections, such as moduli and relative phases between the isoscalar and isovector components from the *BABAR* Collaboration, together with the $\omega\pi$ form factors from the NA60, SND, and CLEO collaborations. The values of resonance couplings, masses and widths of the excited vector states $\rho'$ and $\phi'$ are then determined. The $\omega'$-$\phi'$ mixing angle is discussed and turns out to be quite different from the ideal mixing case. Three sources of $SU(3)$ symmetry breaking effects in the $\Gamma(K^* \to K\gamma)$ decays are identified and analyzed in detail.

## I. INTRODUCTION

The electromagnetic transition form factor of light mesons is one of the key ingredients to study hadron properties, and it has recently gained intensive interest. There are fruitful updated measurements from different experimental collaborations, such as NA60 [1,2], SND [3,4], and *BABAR* [5]. On the theoretical side, the transition form factor provides us with an important tool to study the intrinsic properties of light hadrons, including light pseudoscalar mesons and vector resonances. More importantly, it may also help us to reduce the hadronic uncertainties in the light-by-light scattering, which is an important source of theoretical uncertainties of the muon anomalous magnetic moment [6–8].

The transition form factor of $\pi^0\gamma^*\gamma^*$ is one of the most important form factors in the light-by-light scattering. Physics involved in this kind of form factor is quite complicated since one needs to handle different dynamics within a broad energy region. In the very high and low energy regions, we have reliable and model-independent theoretical tools, namely, pQCD and chiral perturbation theory ($\chi$PT). However, this is not the case in the intermediate energy region, where various resonances enter. In the present work, we follow the chiral effective field theory, explicitly including resonance states developed in Ref. [9] to study the radiative transition form factors involved with vector resonances.

$\chi$PT is a model-independent method to describe the QCD dynamics in the very low energy region ($E \ll M_\rho$), which is based on chiral symmetry and expansions in terms of external momentum and light quark masses [10]. However, the dynamical degrees of freedom in $\chi$PT are restricted to the light pseudo-Goldstone bosons $\pi, K, \eta$ [11]. In the intermediate energy region ($E \sim M_\rho$), clearly the resonance fields need to be explicitly included. References [9,12] proposed an approach to incorporate resonances in a chiral covariant way. In this theory, not only the chiral symmetry but also the QCD inspired high-energy behaviors at large $N_C$ are implemented; thus, the resonance chiral theory (R$\chi$T) has more properties of QCD. Moreover, implementing the high energy constraints in the chiral effective theory also makes it possible to apply the results from this theory directly to some form factors with virtual particles, such as those in light-by-light scattering, where the QCD high energy behavior can be important [7]. At the practical level, imposing the high energy constraints is an efficient way to reduce the number of free resonance couplings, which makes R$\chi$T more predictive in the phenomenological discussions [13–22].

In our previous work [21], we have performed an extensive study on the electromagnetic transition form factors and decays of light pseudoscalar mesons $\pi, \eta, \eta'$ in the framework of R$\chi$T. In the present work, we focus on similar form factors and decays but involving light vector resonances. The relevant resonance operators in these kinds of processes are of the odd-intrinsic-parity type. For the odd-intrinsic-parity sector, Ref. [14] introduced a general effective chiral Lagrangian containing symmetry

---

*Corresponding author.
zhguo@mail.hebtu.edu.cn

allowed interactions between two vector objects (currents or lowest multiplet of resonances) and one pseudoscalar meson, by employing the antisymmetric tensor formalism as used in Ref. [9] to describe the vector resonances. While in Ref. [23], a similar study was carried out, but the vector resonances were described in terms of the Proca vector field representation. Later, the vector-vector-pseudoscalar (VVP) type Lagrangian with vector resonances in the antisymmetric tensor representation has been put forward in different aspects: Reference [17] introduced a second nonet of vector resonances, Ref. [24] worked out the complete basis of resonance operators that are relevant to the $\mathcal{O}(p^6)$ $\chi$PT Lagrangian in the anomaly sector, and in Ref. [21] we have given a comprehensive discussion on the inclusion of the singlet $\eta_1$. Though we have seen impressive progress in this research field, one still needs to bear in mind that in the strict large $N_C$ QCD, there is an infinite tower of zero-width resonances. In practice, typically one has to truncate the tower to the lowest multiplet of resonances, which is called the minimal hadronical ansatz in Ref. [25]. Under this approximation, R$\chi$T has been successfully applied to the phenomenological study on many processes where the intermediate resonances play an important role [15,16,19–21,26–29].

However, we notice that in the previous study of R$\chi$T, most efforts have been made on the lowest lying resonances. For example, in the vector sector, the lowest nonet of $\rho(770)$, $\omega(782)$, $K^*(892)$ and $\phi(1020)$ has been extensively studied, while investigation on the higher mass resonances is relatively rare. One of the important improvements of our present work is to study the excited vector resonances in chiral effective theory, comparing with our previous work [21]. On the experimental side, recently the *BABAR* Collaboration measured the $e^+e^- \to K^*(892)K$ cross sections from the threshold to the energy region around 2–3 GeV [5], which enables us to study properties of more massive vector resonances, i.e., $\rho'$, $\omega'$, and $\phi'$. In this measurement, the moduli and relative phases of isoscalar and isovector components of the $e^+e^- \to K^*(892)K$ cross sections are provided. The updated data make a strong constraint on the free parameters in our theory and hence allow us to accurately extract the resonance properties, such as the masses and widths of the $\rho'$ and $\phi'$ (and also $\omega'$), their mixings, and their couplings to light mesons. The $\omega' - \phi'$ mixing angle is estimated, and we find that it is far from the ideal mixing case.

Another important issue we will address in this article is the $SU(3)$ symmetry breaking effect in radiative decays. An ideal process to study this effect is $K^{*0} \to K^0\gamma$ and $K^{*\pm} \to K^\pm\gamma$. It is well known that the ratio $\frac{\Gamma(K^{*0}\to K^0\gamma)}{\Gamma(K^{*\pm}\to K^\pm\gamma)} = 4$ in the $SU(3)$ limit [30], while the world average value from experimental measurements is around 2.3 [31]. The large $SU(3)$ symmetry breaking effect has been discussed in many previous works [32–36]. In the framework of R$\chi$T, it is interesting to point out that there exists a special

resonance operator $O^4_{\text{VJP}} = \frac{ic_4}{M_V}\epsilon_{\mu\nu\rho\sigma}\langle V^{\mu\nu}[f^{\rho\sigma}_-,\chi_+]\rangle$ [14], which contributes exclusively to the charged processes $K^{*\pm} \to K^\pm\gamma$. Hence, it provides an important source of $SU(3)$ symmetry breaking. In fact, Ref. [16] has determined several values for the $c_4$ parameter in the discussion of hadronic $\tau$ decays. Our present work provides another way to determine its value and allows us to check which kinds of values from Ref. [16] are reasonable. A careful analysis of the strengths of different $SU(3)$ breaking terms $\Gamma(K^{*0} \to K^0\gamma)$ and $\Gamma(K^{*\pm} \to K^\pm\gamma)$ will be delivered in our work.

Contrary to the $K^* \to K\gamma$ process, the $\omega \to \pi^0\gamma^*$ form factor is free of large $SU(3)$ corrections. Nevertheless, another difficulty arises in this form factor, since it is found that the well-established vector-meson-dominant (VMD) model fails to describe $\omega \to \pi^0\gamma^*$ [37–39]. In the present work, we discuss this transition form factor in R$\chi$T by including excited vector resonances in addition to the $\rho(770)$. We will also confront our theoretical results with the new measurements from the SND Collaboration [3,4].

This paper is organized as follows. In Sec. II, we introduce the theoretical framework and elaborate on the calculations for $K^*(892) \to K\gamma$ and $e^+e^- \to K^*(892)K$, the $\omega \to \pi^0\gamma^*$ transition form factor, and the spectral function for $\tau^- \to \omega\pi^-\nu_\tau$. In Sec. III, we present the fit results and discuss the $SU(3)$ symmetry breaking mechanism and the $\omega\pi$ form factors in detail. A summary and conclusions are given in Sec. IV.

## II. THEORETICAL FRAMEWORK

### A. Resonance chiral theory and the odd-intrinsic-parity effective Lagrangian

The low-energy ($\Lambda < m_\rho \approx 700$ MeV) dynamics of QCD is ruled by the interaction of the octet of pseudoscalar mesons, which are characterized by the spontaneous breaking of chiral symmetry. The remarkably successful $\chi$PT [10] describes the strong interactions among pseudoscalar mesons in a model-independent way. The effective Lagrangian to lowest order, $O(p^2)$, is given by

$$\mathcal{L}^{(2)}_\chi = \frac{F^2}{4}\langle u_\mu u^\mu + \chi_+\rangle, \tag{1}$$

where

$$u_\mu = i[u^+(\partial_\mu - ir_\mu)u - u(\partial_\mu - il_\mu)u^+],$$
$$\chi_\pm = u^+\chi u^+ \pm u\chi^+ u, \qquad \chi = 2B_0(s + ip). \tag{2}$$

The unitary matrix in flavor space,

$$u = \exp\left\{i\frac{\Phi}{\sqrt{2}F}\right\}, \tag{3}$$

incorporates the pseudo-Goldstone octet:

$$\Phi = \begin{pmatrix} \frac{1}{\sqrt{2}}\pi^0 + \frac{1}{\sqrt{6}}\eta_8 & \pi^+ & K^+ \\ \pi^- & -\frac{1}{\sqrt{2}}\pi^0 + \frac{1}{\sqrt{6}}\eta_8 & K^0 \\ K^- & \bar{K}^0 & -\frac{2}{\sqrt{6}}\eta_8 \end{pmatrix}. \quad (4)$$

The external sources $r_\mu$, $l_\mu$, $s$, and $p$ promote the global symmetry in the flavor space to a local one. The parameter $F$ corresponds to the pion decay constant $F_\pi = 92.2$ MeV in the chiral limit, and $B_0$ is related to the quark condensate via $\langle 0|\psi\bar{\psi}|0\rangle = -F^2 B_0[1 + O(m_q)]$, with $m_q$ the light quark mass. The explicit chiral symmetry breaking is implemented in $\chi$PT by taking the vacuum expectation values of the scalar sources as $s = \text{Diag}\{m_u, m_d, m_s\}$.

We work in the isospin limit throughout, i.e., taking $m_u = m_d$.

In a chiral covariant way, the lowest multiplet of vector meson resonances was explicitly included in Ref. [9] in terms of antisymmetric tensor fields. In this formalism, the kinetic term of the vector resonance Lagrangian takes the form

$$\mathcal{L}_{\text{kin}}(V) = -\frac{1}{2}\left\langle \nabla^\lambda V_{\lambda\mu}\nabla_\nu V^{\nu\mu} - \frac{M_V^2}{2}V_{\mu\nu}V^{\mu\nu}\right\rangle, \quad (5)$$

with the ground vector nonet

$$V_{\mu\nu} = \begin{pmatrix} \frac{1}{\sqrt{2}}\rho^0 + \frac{1}{\sqrt{6}}\omega_8 + \frac{1}{\sqrt{3}}\omega_1 & \rho^+ & K^{*+} \\ \rho^- & -\frac{1}{\sqrt{2}}\rho^0 + \frac{1}{\sqrt{6}}\omega_8 + \frac{1}{\sqrt{3}}\omega_1 & K^{*0} \\ K^{*-} & \bar{K}^{*0} & -\frac{2}{\sqrt{6}}\omega_8 + \frac{1}{\sqrt{3}}\omega_1 \end{pmatrix}_{\mu\nu}, \quad (6)$$

and the covariant derivative and the chiral connection defined as

$$\nabla_\mu V = \partial_\mu V + [\Gamma_\mu, V],$$
$$\Gamma_\mu = \frac{1}{2}\{u^+(\partial_\mu - ir_\mu)u + u(\partial_\mu - il_\mu)u^+\}. \quad (7)$$

At leading order of $1/N_C$, the mass splitting of the ground vector multiplet is governed by a single resonance operator [40]

$$-\frac{1}{2}e_m^V\langle V_{\mu\nu}V^{\mu\nu}\chi_+\rangle. \quad (8)$$

In Ref. [41], it was demonstrated that this single operator can explain the mass splittings of $\rho(770)$, $K^*(895)$, and $\phi(1020)$ well. In addition to the mass splittings of these vector resonances, this operator is also shown to be able to perfectly reproduce the quark mass dependence of the $\rho(770)$ mass from the lattice simulation [42]. We will then employ the single operator in Eq. (8) to account for the mass splittings of the lowest vector multiplet in this work. Additional $1/N_C$ suppressed operators, such as $\langle V_{\mu\nu}\rangle\langle V^{\mu\nu}\rangle$, will not be considered for the well-established ground vectors, due to the fact that $\omega(782)$ and $\phi(1020)$ in the ground multiplet are well described by the ideal mixing between the octet and singlet vector states. However, because of the unclear situation for the excited vectors, the $1/N_C$ suppressed operators will be introduced later. Combining Eqs. (5) and (8), it can be easily verified that the

physical states of $\omega(782)$ and $\phi(1020)$ result from the ideal mixing of $\omega_1$ and $\omega_8$,

$$\omega_1 = \sqrt{\frac{2}{3}}\omega - \sqrt{\frac{1}{3}}\phi, \qquad \omega_8 = \sqrt{\frac{2}{3}}\phi + \sqrt{\frac{1}{3}}\omega. \quad (9)$$

Then the mass splitting pattern of the ground vector multiplet takes the form

$$M_\rho^2 = M_\omega^2 = M_V^2 - 4e_m^V m_\pi^2,$$
$$M_{K^*}^2 = M_V^2 - 4e_m^V m_K^2,$$
$$M_\phi^2 = M_V^2 - 4e_m^V(2m_K^2 - m_\pi^2), \quad (10)$$

where we have used the leading order relations $2m_u B_0 = m_\pi^2$ and $(m_u + m_s)B_0 = m_K^2$.

For the general interaction Lagrangian linear in $V_{\mu\nu}$ up to $O(p^2)$, it reads [9]

$$\mathcal{L}_2(V) = \frac{F_V}{2\sqrt{2}}\langle V_{\mu\nu}f_+^{\mu\nu}\rangle + \frac{iG_V}{\sqrt{2}}\langle V_{\mu\nu}u^\mu u^\nu\rangle, \quad (11)$$

$$f_\pm^{\mu\nu} = uF_L^{\mu\nu}u^+ \pm u^+ F_R^{\mu\nu}u, \quad (12)$$

with $F_{L,R}^{\mu\nu}$ the field strength tensors of the left and right external sources $l_\mu$ and $r_\mu$, respectively. $F_V$ and $G_V$ are real resonance coupling constants, and only $F_V$ is relevant in our current study.

The interaction operators containing two-vector and one-pseudoscalar objects have been worked out in Ref. [14],

$$\mathcal{L}_{\text{VJP}} = \frac{c_1}{M_V}\epsilon_{\mu\nu\rho\sigma}\langle\{V^{\mu\nu}, f_+^{\rho\alpha}\}\nabla_\alpha u^\sigma\rangle + \frac{c_2}{M_V}\epsilon_{\mu\nu\rho\sigma}\langle\{V^{\mu\alpha}, f_+^{\rho\sigma}\}\nabla_\alpha u^\nu\rangle + \frac{ic_3}{M_V}\epsilon_{\mu\nu\rho\sigma}\langle\{V^{\mu\nu}, f_+^{\rho\sigma}\}\chi_-\rangle$$

$$+ \frac{ic_4}{M_V}\epsilon_{\mu\nu\rho\sigma}\langle V^{\mu\nu}[f_-^{\rho\sigma},\chi_+]\rangle + \frac{c_5}{M_V}\epsilon_{\mu\nu\rho\sigma}\langle\{\nabla_\alpha V^{\mu\nu}, f_+^{\rho\alpha}\}u^\sigma\rangle + \frac{c_6}{M_V}\epsilon_{\mu\nu\rho\sigma}\langle\{\nabla_\alpha V^{\mu\alpha}, f_+^{\rho\sigma}\}u^\nu\rangle$$

$$+ \frac{c_7}{M_V}\epsilon_{\mu\nu\rho\sigma}\langle\{\nabla^\sigma V^{\mu\nu}, f_+^{\rho\alpha}\}u_\alpha\rangle, \tag{13}$$

$$\mathcal{L}_{\text{VVP}} = d_1\epsilon_{\mu\nu\rho\sigma}\langle\{V^{\mu\nu}, V^{\rho\alpha}\}\nabla_\alpha u^\sigma\rangle + id_2\epsilon_{\mu\nu\rho\sigma}\langle\{V^{\mu\nu}, V^{\rho\sigma}\}\chi_-\rangle$$

$$+ d_3\epsilon_{\mu\nu\rho\sigma}\langle\{\nabla_\alpha V^{\mu\nu}, V^{\rho\alpha}\}u^\sigma\rangle + d_4\epsilon_{\mu\nu\rho\sigma}\langle\{\nabla^\sigma V^{\mu\nu}, V^{\rho\alpha}\}u_\alpha\rangle, \tag{14}$$

with $\epsilon_{\mu\nu\rho\sigma}$ the Levi-Civita antisymmetric tensor. Similar operators with an excited vector multiplet $V_1$ can be straightforwardly constructed [17],

$$\mathcal{L}_2(V_1) = \frac{F_{V_1}}{2\sqrt{2}}\langle V_{1\mu\nu}f_+^{\mu\nu}\rangle, \tag{15}$$

$$\mathcal{L}_{VV_1P} = d_a\epsilon_{\mu\nu\rho\sigma}\langle\{V^{\mu\nu}, V_1^{\rho\alpha}\}\nabla_\alpha u^\sigma\rangle + d_b\epsilon_{\mu\nu\rho\sigma}\langle\{V^{\mu\alpha}, V_1^{\rho\sigma}\}\nabla_\alpha u^\nu\rangle + d_c\epsilon_{\mu\nu\rho\sigma}\langle\{\nabla_\alpha V^{\mu\nu}, V_1^{\rho\alpha}\}u^\sigma\rangle$$

$$+ d_d\epsilon_{\mu\nu\rho\sigma}\langle\{\nabla_\alpha V^{\mu\alpha}, V_1^{\rho\sigma}\}u^\nu\rangle + d_e\epsilon_{\mu\nu\rho\sigma}\langle\{\nabla^\sigma V^{\mu\nu}, V_1^{\rho\alpha}\}u_\alpha\rangle + id_f\epsilon_{\mu\nu\rho\sigma}\langle\{V^{\mu\nu}, V_1^{\rho\sigma}\}\chi_-\rangle. \tag{16}$$

The kinetic Lagrangian for the excited vector takes the same form as that in Eq. (5). The operators equivalent to Eq. (13) involving the excited vector multiplet $V_1$ happen to be irrelevant to the discussions in the present article.

For later convenience, we follow the convention introduced in Ref. [19] to define certain combinations of $d_i$ in Eq. (16),

$$d_m = d_a + d_b - d_c + 8d_f,$$
$$d_M = d_b - d_a + d_c - 2d_d,$$
$$d_s = d_c + d_a - d_b. \tag{17}$$

In the present article, since we focus on the processes involving the pion and kaon, the additional operators that we introduced in Ref. [21] to discuss $\eta$ and $\eta'$ will be irrelevant. So we do not elaborate more on this issue. The flavor structure for the excited vector multiplet $V_1$ is the same as the ground multiplet in Eq. (6). However, unlike the well-established entries in the ground vector multiplet, the contents of the excited vector multiplet are still not clear. Therefore, we include a general set of mass splitting operators to describe the excited vectors, instead of only using a single operator in the ground multiplet case. Up to the linear quark mass corrections, the pertinent operators read [40]

$$\mathcal{L}_{V_1}^{\text{mass-split}} = -\frac{1}{2}\left(e_m^{V_1}\langle V_{1\mu\nu}V_1^{\mu\nu}\chi_+\rangle - \frac{\gamma_{V_1}M_{V_1}^2}{2}\langle V_{1\mu\nu}\rangle\langle V_1^{\mu\nu}\rangle\right), \tag{18}$$

where the second operator is $1/N_C$ suppressed compared to the first one and $M_{V_1}$ is the mass of the excited vector multiplet in the chiral limit. Another type of operator, e.g., $-1/(2\sqrt{3})k_m^{V_1}\langle V_{1\mu\nu}\rangle\langle\hat{V}_1^{\mu\nu}\chi_+\rangle$, was also introduced in

Ref. [40], but we consider this operator to be less relevant compared to the two terms in Eq. (18). The reason for this is that compared to the $e_m^{V_1}$ term, though the $\gamma_{V_1}$ term is $1/N_C$ suppressed, its chiral order is enhanced, while for the $k_m^{V_1}$ term, its chiral and $1/N_C$ orders are both suppressed.

Owing to the $1/N_C$ suppressed operator in Eq. (18), the excited states $\omega'$ and $\phi'$ cannot be simply described as the ideal mixing of $\omega_1'$ and $\omega_8'$ as in the ground-state case. The physical states of $\omega'$ and $\phi'$ are related to the octet-singlet basis through

$$\omega' = \sin\theta_V\omega_8' + \cos\theta_V\omega_1',$$
$$\phi' = \cos\theta_V\omega_8' - \sin\theta_V\omega_1'. \tag{19}$$

The mixing angle $\theta_V$ and the masses of $\omega'$ and $\phi'$ can be expressed in terms of the couplings in Lagrangian (18),

$$M_{\omega'}^2 = \frac{M_{11}^2 + M_{22}^2 - \sqrt{(M_{11} - M_{22})^2 + 4M_{12}^2}}{2}, \tag{20}$$

$$M_{\phi'}^2 = \frac{M_{11}^2 + M_{22}^2 + \sqrt{(M_{11} - M_{22})^2 + 4M_{12}^2}}{2}, \tag{21}$$

$$\sin\theta_V = -\frac{M_{12}^2}{\sqrt{(M_{\phi'}^2 - M_{\omega'}^2)(M_{11}^2 - M_{\omega'}^2)}}, \tag{22}$$

with

$$M_{11}^2 = M_{V_1}^2 - \frac{4}{3}e_m^{V_1}(4m_K^2 - m_\pi^2), \tag{23}$$

$$M_{22}^2 = M_{V_1}^2(1 + \gamma_{V_1}) - \frac{4}{3}e_m^{V_1}(2m_K^2 + m_\pi^2), \tag{24}$$

$$M_{12}^2 = \frac{8\sqrt{2}}{3}e_m^{V_1}(m_K^2 - m_\pi^2). \tag{25}$$

However, for the masses of $\rho'$ and $K^{*'}$, only the $e_m^{V_1}$ term in Eq. (18) contributes, and they take the same form as the ground states in Eq. (10),

$$M_{\rho'}^2 = M_{V_1}^2 - 4e_m^{V_1} m_\pi^2, \tag{26}$$

$$M_{K^{*'}}^2 = M_{V_1}^2 - 4e_m^{V_1} m_K^2. \tag{27}$$

Including the quark mass corrections to the resonance masses in the Lagrangian approach allows us to incorporate the $SU(3)$ symmetry breaking effects in a systematic way. This is important to understand the $SU(3)$ symmetry breaking mechanism in the $K^*K$ transitions. The quark mass corrections to the resonance masses, as well as to interacting vertices, are important to fully study the $SU(3)$ symmetry breaking effects. The VVP-type Lagrangians introduced in Eqs. (13), (14), and (16), which are constructed by using the chiral building blocks of the pseudo-Goldstone mesons, provide us with an appropriate framework to systematically take into account the relevant interacting vertices. Though it consists of a large number of free couplings, we will see later that in a given process not all of them are independent. In fact, in our present discussion, only six, at most, of the combinations of the VVP-type couplings will appear after taking into account the high energy constraints dictated by QCD.

Imposing the high energy constraints will not only give the RχT more properties from QCD, but it will also be helpful in reducing the number of free parameters. To proceed, we match the leading operator product expansion (OPE) of the VVP Green function with the result evaluated within RχT, and we require that the vector form factor vanish in the high energy limit. This leads to the following constraints on resonance couplings:

$$4c_3 + c_1 = 0,$$

$$c_1 - c_2 + c_5 = 0,$$

$$c_6 - c_5 = \frac{2d_3 F_V + d_s F_{V_1}}{2\sqrt{2} M_V}, \tag{28}$$

which were already given by one of us in Ref. [19]. We point out that the previous constraints are obtained in the chiral and large $N_C$ limits, as done in most of the RχT studies [13–22] in the literature.

### B. The transition amplitudes of $K^* \longrightarrow K\gamma$ decays and $e^+e^- \longrightarrow K^*K$ processes

At leading order of $1/N_C$ in RχT, the $V \longrightarrow P\gamma(\gamma^*)$ transitions receive two types of contributions, as displayed in Fig. 1, namely, the direct type depicted by diagram (a) and the indirect one depicted by diagram (b).

The structure of the amplitude for the $K^*(q) \to K + \gamma(k)$ process can be written as

$$iM_{K^*K\gamma} \equiv i\epsilon_{\mu\nu\rho\sigma} \epsilon_{K^*}^\mu \epsilon_\gamma^\nu q^\rho k^\sigma e g_{K^*K\gamma}^{\text{total}},$$

$$g_{K^*K\gamma}^{\text{total}} = g_{K^*K\gamma}^{\text{direct}} + g_{K^*K\gamma}^{\text{indirect}}, \tag{29}$$

where $q$ and $k$ denote the four-momenta of $K^*$ and $\gamma$, respectively, $\epsilon_{K^*}$ and $\epsilon_\gamma$ correspond to the polarization vectors in that order, and $e$ stands for the electric charge of a positron. In the previous equation, we collect the contributions from the direct and indirect diagrams of Fig. 1 in the quantities $g_{K^*K\gamma}^{\text{direct}}$ and $g_{K^*K\gamma}^{\text{indirect}}$, respectively.

By using the previously introduced resonance Lagrangian in Sec. II A, it is straightforward to calculate $g_{K^*K\gamma}^{\text{direct}}$ and $g_{K^*K\gamma}^{\text{indirect}}$:

$$g_{K^{*0}K^0\gamma}^{\text{direct}} = -\frac{4\sqrt{2}}{3F_K M_V M_{K^*}} [(c_1 + c_2 + 8c_3 - c_5)m_K^2 + (c_2 + c_5 - c_1 - 2c_6)M_{K^*}^2],$$

$$g_{K^{*0}K^0\gamma}^{\text{indirect}} = -\frac{2F_V}{3F_K M_{K^*}} \left(\frac{1}{M_\omega^2} - \frac{3}{M_\rho^2} - \frac{2}{M_\phi^2}\right)[(d_1 + 8d_2 - d_3)m_K^2 + d_3 M_{K^*}^2],$$

$$- \frac{F_{V_1}}{3F_K M_{K^*}} \left[\frac{(2\sqrt{2}\cos\theta_V - \sin\theta_V)\sin\theta_V}{M_{\omega'}^2} - \frac{3}{M_{\rho'}^2} - \frac{(\cos\theta_V + 2\sqrt{2}\sin\theta_V)\cos\theta_V}{M_{\phi'}^2}\right]$$

$$\times (d_m m_K^2 + d_M M_{K^*}^2), \tag{30}$$

$$g_{K^{*+}K^+\gamma}^{\text{direct}} = \frac{2\sqrt{2}}{3F_K M_V M_{K^*}} [(c_1 + c_2 + 8c_3 - c_5)m_K^2 + (c_2 + c_5 - c_1 - 2c_6)M_{K^*}^2$$

$$+ 24c_4(m_K^2 - m_\pi^2)],$$

$$g_{K^{*+}K^+\gamma}^{\text{indirect}} = -\frac{2F_V}{3F_K M_{K^*}} \left(\frac{1}{M_\omega^2} + \frac{3}{M_\rho^2} - \frac{2}{M_\phi^2}\right)[(d_1 + 8d_2 - d_3)m_K^2 + d_3 M_{K^*}^2]$$

$$- \frac{F_{V_1}}{3F_K M_{K^*}} \left[\frac{(2\sqrt{2}\cos\theta_V - \sin\theta_V)\sin\theta_V}{M_{\omega'}^2} + \frac{3}{M_{\rho'}^2} - \frac{(\cos\theta_V + 2\sqrt{2}\sin\theta_V)\cos\theta_V}{M_{\phi'}^2}\right]$$
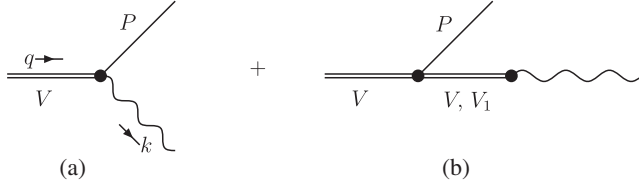
$$\times (d_m m_K^2 + d_M M_{K^*}^2). \tag{31}$$

FIG. 1. Diagrams relevant to the $V \to P\gamma(\gamma^*)$ processes: (a) direct type and (b) indirect type.

Physical meson masses are used in the kinematics. The kaon decay constant $F_K$ has been employed in the amplitude, instead of the pseudo-Goldstone decay constant $F$ in the chiral limit that appears in the resonance chiral Lagrangian. We take $F_K = 0.113$ GeV from particle data group (PDG) [31].

Within our formalism, the $\Gamma(K^* \to K\gamma)$ decay width is given by

$$\Gamma(K^* \to K\gamma) = \frac{1}{3}\alpha\left(\frac{M_{K^*}^2 - m_K^2}{2M_{K^*}}\right)^3 |g_{K^*K\gamma}^{\text{total}}|^2, \quad (32)$$

with $\alpha = e^2/(4\pi)$ the fine-structure constant.

In the leading order of large $N_C$, the $e^+e^- \to K^*(892)K$ transition also receives two types of contributions, i.e., direct and indirect types, as displayed in Fig. 2.

The main difference between $e^+e^- \to K^*(892)K$ and $K^* \to K\gamma$ is that now we have an off-shell photon. The final results for the amplitudes of $\gamma^* \longrightarrow K^*K$ can be obtained in the same way as in the $K^* \to K\gamma$ case. In order to confront our theoretical results with the experimental data, we need to work in the isospin bases for the amplitudes,

$$
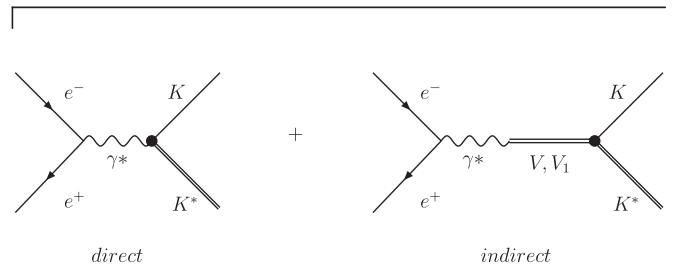\begin{aligned}
iM_{I=0} &= i\frac{\sqrt{2}}{2}(M_{\gamma^* \longrightarrow K^{*+}K^-} + M_{\gamma^* \longrightarrow \bar{K}^{*0}K^0}) \\
&= i\epsilon_{\alpha\beta\rho\sigma}\epsilon_{K^*}^\alpha \epsilon_\gamma^\beta q^\rho k^\sigma e \frac{\sqrt{2}}{2}\frac{1}{F_K M_{K^*}}\left\{-\frac{2\sqrt{2}}{3M_V}[(c_1 + c_2 + 8c_3 - c_5)M_K^2 + (c_2 + c_5 - c_1 - 2c_6)M_{K^*}^2 \right. \\
&\quad + (c_1 - c_2 + c_5)s - 24c_4(m_K^2 - m_\pi^2)] - 4F_V\left[\frac{1}{3(M_\omega^2 - s - iM_\omega\Gamma_\omega)} - \frac{2}{3(M_\phi^2 - s - iM_\phi\Gamma_\phi)}\right] \\
&\quad \times [(d_1 + 8d_2)m_K^2 + d_3(M_{K^*}^2 + s - m_K^2)] - 2F_{V_1}\left[\frac{(2\sqrt{2}\cos\theta_V - \sin\theta_V)\sin\theta_V}{3(M_{\omega'}^2 - s - iM_{\omega'}\Gamma_{\omega'}(s))}\right. \\
&\quad \left.\left. - \frac{(\cos\theta_V + 2\sqrt{2}\sin\theta_V)\cos\theta_V}{3(M_{\phi'}^2 - s - iM_{\phi'}\Gamma_{\phi'}(s))}\right](d_m m_K^2 + d_M M_{K^*}^2 + d_s s)\right\} \\
&\triangleq i\epsilon_{\alpha\beta\rho\sigma}\epsilon_{K^*}^\alpha \epsilon_\gamma^\beta q^\rho k^\sigma eA_0, \quad (33)
\end{aligned}
$$

$$
\begin{aligned}
iM_{I=1} &= i\frac{\sqrt{2}}{2}(M_{\gamma^* \longrightarrow \bar{K}^{*0}K^0} - M_{\gamma^* \longrightarrow K^{*+}K^-}) \\
&= i\epsilon_{\alpha\beta\rho\sigma}\epsilon_{K^*}^\alpha \epsilon_\gamma^\beta q^\rho k^\sigma e \frac{\sqrt{2}}{2}\frac{1}{F_K M_{K^*}}\left\{-\frac{2\sqrt{2}}{M_V}[(c_1 + c_2 + 8c_3 - c_5)M_K^2 + (c_2 + c_5 - c_1 - 2c_6)M_{K^*}^2 \right. \\
&\quad + (c_1 - c_2 + c_5)s + 8c_4(m_K^2 - m_\pi^2)] + 4F_V\frac{1}{M_\rho^2 - s - iM_\rho\Gamma_\rho(s)}[(d_1 + 8d_2)m_K^2 \\
&\quad \left. + d_3(M_{K^*}^2 + s - m_K^2)] + 2F_{V_1}\frac{1}{M_{\rho'}^2 - s - iM_{\rho'}\Gamma_{\rho'}(s)}(d_m m_K^2 + d_M M_{K^*}^2 + d_s s)\right\} \\
&\triangleq i\epsilon_{\alpha\beta\rho\sigma}\epsilon_{K^*}^\alpha \epsilon_\gamma^\beta q^\rho k^\sigma eA_1, \quad (34)
\end{aligned}
$$

where $q$ and $k$ stand for the momenta of $K^*$ and $\gamma^*$, respectively, and $s = k^2$ is the energy square of the $e^+e^-$ system in the center-of-mass frame. The energy-dependent decay widths for intermediate resonances, such as $\Gamma_\rho(s), \Gamma_{\rho'}(s), \Gamma_{\phi'}(s)$, and $\Gamma_{\omega'}(s)$, can be important since the widths of the relevant resonances are typically not so narrow and the final results can be sensitive to the off-shell width effects. To rigorously include the off-shell



FIG. 2. Relevant diagrams for the process $e^+e^- \longrightarrow K^*(892)K$.

width effects, one needs to carry out the next-to-leading order of $1/N_C$ computation in R$\chi$T, which is beyond the scope of this work since we focus on the calculations of the various amplitudes at leading order of $1/N_C$. Nevertheless, in order to quantitatively estimate to what extent the off-shell width effects will affect the final outputs, we study two different forms of the energy-dependent widths, which will be discussed in detail in the next section.

We see that only the $\omega$-like and $\phi$-like intermediate mesons contribute to the $M_{I=0}$, and only the $\rho$-like intermediate mesons contribute to the $M_{I=1}$. However, the local terms or the so-called background terms in many other works [5] are obtained here from a Lagrangian-based theory, not simply introduced by hand. The cross sections are related to the isospin amplitudes through

$$\sigma_{e^+e^- \longrightarrow K^*K(I=0,1)} = \frac{\pi\alpha^2|A_{I=0,1}|^2}{6s^3}(s^2 + M_{K^*}^4 + m_K^4$$
$$- 2sM_{K^*}^2 - 2sm_K^2 - 2M_{K^*}^2m_K^2)^{\frac{3}{2}}, \tag{35}$$

where the masses of the electron and positron have been neglected.

## C. The $\omega \longrightarrow \pi^0\gamma^*$ transition form factor and the spectral function for $\tau^- \to \omega\pi^-\nu_\tau$

The amplitude for the radiative decay $\omega(q) \to \pi^0(p)\gamma^*(k)$ can be written as

$$i\mathcal{M}_{\omega \to \pi^0\gamma^*} = ie\varepsilon_{\mu\nu\rho\sigma}\epsilon_\omega^\mu\epsilon_{\gamma^*}^\nu q^\rho k^\sigma f_{\omega\pi^0}(s), \tag{36}$$

where $s = k^2$, and $\epsilon_\omega$ and $\epsilon_{\gamma^*}$ denote the polarization vectors of the $\omega$ resonance and the off-shell photon, respectively. The explicit expression of the electromagnetic transition form factor $f_{\omega\pi^0}(s)$ is

$$f_{\omega\pi^0}(s) = -\frac{2\sqrt{2}}{F_\pi M_V M_\omega}[(c_1 + c_2 + 8c_3 - c_5)m_\pi^2 + (c_2 + c_5 - c_1 - 2c_6)M_\omega^2 + (c_1 - c_2 + c_5)s]$$
$$+ \frac{4F_V}{F_\pi M_\omega}\frac{1}{M_\rho^2 - s - iM_\rho\Gamma_\rho(s)}[(d_1 + 8d_2 - d_3)m_\pi^2 + d_3(M_\omega^2 + s)]$$
$$+ \frac{2F_{V_1}}{F_\pi M_\omega}\frac{1}{M_{\rho'}^2 - s - iM_{\rho'}\Gamma_{\rho'}(s)}[d_M M_\omega^2 + d_s s + d_m m_\pi^2]. \tag{37}$$

In the phenomenological discussion, it is common to normalize the form factor $f_{\omega\pi^0}(s)$ by its value at $s = 0$. So the interesting quantity that we will study later is

$$F_{\omega\pi^0}(s) = \frac{f_{\omega\pi^0}(s)}{f_{\omega\pi^0}(0)}. \tag{38}$$

The charged $\omega\pi$ form factor or the $\omega\pi$ spectral function can be measured in the semileptonic decays of the $\tau$ lepton. In Eq. (35) of Ref. [19], one of us calculated the $\tau^- \to \omega\pi^-\nu_\tau$ spectral function. We give the explicit expression here for completeness:

$$V(s) = \frac{1}{6F^2 M_\omega^2 \pi s^2 S_{EW}} \times [m_\pi^4 + (M_\omega^2 - s)^2 - 2m_\pi^2(M_\omega^2 - s)]^{3/2}$$
$$\times \left|(2d_3F_V + d_sF_{V_1})\frac{M_\omega^2}{M_V^2} + F_{V_1}(d_m m_\pi^2 + d_M M_\omega^2 + d_s s)\frac{1}{M_{\rho'}^2 - s - iM_{\rho'}\Gamma_{\rho'}(s)}\right.$$
$$\left. + 2F_V[(d_1 + 8d_2)m_\pi^2 + d_3(s + M_\omega^2 - m_\pi^2)]\frac{1}{M_\rho^2 - s - iM_\rho\Gamma_\rho(s)}\right|^2, \tag{39}$$

where the electroweak correction factor $S_{EW}$ has been analyzed in [43], and its value will be taken as $S_{EW} = 1.0194$.

## III. PHENOMENOLOGICAL DISCUSSIONS

### A. The fit results

The experimental data that we consider here consist of eight different types: $\Gamma(K^{*0} \to K^0\gamma)$ [31], $\Gamma(K^{*+} \to K^+\gamma)$ [31], the $e^+e^- \to K^{*\pm}(892)K^\mp$ cross sections [5], the moduli and relative phases of isoscalar and isovector components of the $e^+e^- \to K^*(892)K$ cross sections [5], the $\omega \to \pi^0\gamma^*$ transition form factor [1–4,44], and the $\tau^- \to \omega\pi^-\nu_\tau$ spectral function [45].

For the $e^+e^- \to K^*(892)K$ data in Ref. [5], since in the energy region above 1.8 GeV the contributions coming from other excited vector resonances with higher mass and spin certainly affect the $KK^*(892)$ channel, we only fit the data below 1.8 GeV. For the $\omega'$ [$\omega(1420)$], we fix its mass and width at their world average values, $M_{\omega'} = 1.42$ GeV and $\Gamma_{\omega'} = 0.215$ GeV [31], because its mass is quite close to the $K^*K$ threshold and its contribution only marginally shows up in the left tail of the $e^+e^- \to K^*(892)K$ cross sections.

Due to the fact that the masses of the ground vector resonances, $\rho, \omega, \phi, K^*$, can be perfectly described by Eq. (10) (see Refs. [41,42]), we simply employ the physical masses of $\rho, \omega, \phi, K^*$ in the numerical discussions, instead of fitting the $e_m^V$ coupling. We point out that if the value of $e_m^V$ is fitted, it turns out to be very close to the values given in Refs. [41,42]. For the mass of the ground vector in the chiral limit, we take the value $M_V = 764.3$ MeV from Ref. [41]. As to the value of $F_V$, it has been accurately determined by taking into account a large amount of experimental data in our previous work [21]. Hence, we will take the value from that reference in this work, which is $F_V = 0.137$ GeV. For $F_{V_1}$ in Eq. (15), since what appears in our discussion is always the combination of $F_{V_1}(d_m m_K^2 + d_M M_{K^*}^2)$ or $F_{V_1}(d_m m_K^2 +$

$d_M M_{K^*}^2 + d_s s)$, which was already noticed in Ref. [19], we can fix the sign of $F_{V_1}$ and leave $d_m, d_M$, and $d_s$ free. In Ref. [19], $F_{V_1} = -0.1$ GeV has been determined, and we will take this value in our current study.

As mentioned previously, we introduce the finite-width effects to the intermediate resonances. To systematically include the finite-width contributions in R$\chi$T, one has to step into the next-to-leading order of $1/N_C$ computation, e.g., the one-loop calculations, which is far beyond the scope of our study. Nevertheless, we will employ two different parametrizations for the energy-dependent widths for the broad resonances in order to see how important the off-shell width effects will affect the fit results. For the narrow-width resonances, such as $\omega$ and $\phi$, we simply use the constant widths in their propagators.

For the first case, which will be referred to as Fit I in later discussions, we construct the energy-dependent widths for broad resonances following the approach given in Ref. [46], where the authors have taken the chiral symmetry, analyticity, and unitarity into account when discussing the form of the off-shell width for the $\rho(770)$ resonance. The result of the previous reference has been generalized to other resonances in many phenomenological discussions [15,19,21,47]. In this formalism, we construct the energy-dependent widths in the following way:

$$\Gamma_\rho(s) = \frac{sM_\rho}{96\pi F_\pi^2}\left[\sigma_{\pi\pi}^3(s) + \frac{1}{2}\sigma_{KK}^3(s)\right],$$

$$\Gamma_{\rho'}(s) = \Gamma_{\rho'}\frac{s}{M_{\rho'}^2}\left[\frac{\sigma_{\pi\pi}^3(s) + \frac{1}{2}\sigma_{KK}^3(s)}{\sigma_{\pi\pi}^3(M_{\rho'}^2) + \frac{1}{2}\sigma_{KK}^3(M_{\rho'}^2)}\right],$$

$$\Gamma_{\omega'}(s) = \Gamma_{\omega'}\frac{s}{M_{\omega'}^2}\left[\frac{\sigma_{\rho\pi}^3(s) + \frac{(2\sqrt{2}\cos\theta_V - \sin\theta_V)^2}{3(\sqrt{2}\cos\theta_V + \sin\theta_V)^2}\sigma_{K^*K}^3(s)}{\sigma_{\rho\pi}^3(M_{\omega'}^2) + \frac{(2\sqrt{2}\cos\theta_V - \sin\theta_V)^2}{3(\sqrt{2}\cos\theta_V + \sin\theta_V)^2}\sigma_{K^*K}^3(M_{\omega'}^2)}\right],$$

$$\Gamma_{\phi'}(s) = \Gamma_{\phi'}\frac{s}{M_{\phi'}^2}\left[\frac{\sigma_{K^*K}^3(s) + \frac{4(\sqrt{2}\cos\theta_V + \sin\theta_V)^2}{3(\cos\theta_V + 2\sqrt{2}\sin\theta_V)^2}\sigma_{\phi\eta}^3(s)}{\sigma_{K^*K}^3(M_{\phi'}^2) + \frac{4(\sqrt{2}\cos\theta_V + \sin\theta_V)^2}{3(\cos\theta_V + 2\sqrt{2}\sin\theta_V)^2}\sigma_{\phi\eta}^3(M_{\phi'}^2)}\right], \tag{40}$$

where

$$\sigma_{QR}(s) = \frac{1}{s}\sqrt{(s - (m_Q + m_R)^2)(s - (m_Q - m_R)^2)}$$
$$\times \theta(s - (m_Q + m_R)^2), \tag{41}$$

with $\theta(s)$ the standard step function.

In Fit II, we take a different asymptotic behavior for the energy-dependent widths compared to that used in Fit I,

$$\Gamma_R(s) = \Gamma_R^I(s)\frac{M_R}{\sqrt{s}}, \quad R = \rho, \rho', \omega', \phi', \tag{42}$$

with $\Gamma_R^I(s)$ defined in Eq. (40). In the asymptotic region where $s \to \infty$, the power of the energy-dependent width

should be less than 1, in such a way that the phase of the amplitudes in Eqs. (33) and (34) would approach $\pi$. In Fit I, we adopt the results from Ref. [46], where only $\pi\pi$ and $\bar{K}K$ channels are considered when deriving the finite width for $\rho(770)$. In principle, an infinite number of channels will be open when $s \to \infty$, which could finally alternate the asymptotic behaviors obtained by considering a finite number of channels. A definite answer to this problem clearly deserves an independent work. As a phenomenological study, we will exploit both forms to perform the fits and examine to what extent different forms can affect the final outputs.

The values for the fit parameters are summarized in Table I. The results of $\Gamma(K^{*0} \to K^0\gamma)$, $\Gamma(K^{*+} \to K^+\gamma)$, and

TABLE I.   The parameter results from Fit I and Fit II.

|  | Fit I | Fit II |
|---|---|---|
| $M_{V_1}$ | $1587 \pm 7$ | $1523 \pm 5$ |
| $e_m^{V_1}$ | $-0.262 \pm 0.014$ | $-0.329 \pm 0.010$ |
| $\gamma_{V_1}$ | $-0.246 \pm 0.006$ | $-0.180 \pm 0.006$ |
| $\Gamma_{\rho'}$ (MeV) | $545 \pm 22$ | $433 \pm 13$ |
| $\Gamma_{\phi'}$ (MeV) | $266 \pm 17$ | $210 \pm 11$ |
| $c_4$ | $-0.0023 \pm 0.0006$ | $-0.0024 \pm 0.0005$ |
| $d_3$ | $-0.198 \pm 0.004$ | $-0.191 \pm 0.004$ |
| $d_M$ | $-0.38 \pm 0.10$ | $-0.21 \pm 0.08$ |
| $d_s$ | $-0.13 \pm 0.02$ | $-0.12 \pm 0.02$ |
| $d_m$ | $-1.79 \pm 0.15$ | $-1.22 \pm 0.12$ |
| $d_1 + 8d_2$ | $-0.38 \pm 0.04$ | $-0.36 \pm 0.04$ |
| $\frac{\chi^2}{\text{d.o.f}}$ | $\frac{467.7}{210-11} = 2.35$ | $\frac{589.1}{210-11} = 2.96$ |
| Results for $V_1$ |  |  |
| $M_{\rho'}$ (MeV) | $1593 \pm 8$ | $1531 \pm 8$ |
| $M_{\phi'}$ (MeV) | $1709 \pm 7$ | $1690 \pm 6$ |
| $M_{K^{*'}}$ (MeV) | $1667 \pm 6$ | $1626 \pm 7$ |
| $\theta_V$ | $15.1° \pm 2.0°$ | $21.3° \pm 2.2°$ |

$\frac{\Gamma(K^{*0} \to K^0 \gamma)}{\Gamma(K^{*+} \to K^+ \gamma)}$ from the fits are given in Table II. The final results corresponding to the $e^+ e^- \to K^*(892) K$ processes and the $\omega \pi$ spectral function from $\tau^- \to \omega \pi^- \nu_\tau$ are shown in Figs. 3 and 4, respectively. In these two figures, we distinguish different results from Fit I and Fit II by solid and dashed lines, respectively. The resulting curves for the $\omega \to \pi^0 \gamma^*$ form factors are plotted in Fig. 5, together with the results from Refs. [48,49].

Some comments about the fitting results are given below.

First, we observe that Fit I is slightly preferred over Fit II, according to the values of $\chi^2$/degrees of freedom (d.o.f.). Nevertheless, due to the fact that the values of $\chi^2$/d.o.f. are already bigger than 2, the preference is not really significant. Regarding the somewhat large values of $\chi^2$/d.o.f., we find that they are mainly contributed by the $\omega \to \pi \gamma^*$ form factors from the NA60 and Lepton-G measurements, especially from the data points in the energy region around 0.5–0.63 GeV. Therefore, we have tried another kind of fit to exclude the data from these two measurements. It turns out that the resulting values of $\chi^2$/d.o.f. decrease to around 1.2 in Fit I and to 1.9 in Fit II, and we do not observe significant changes of the fit parameters compared with the

TABLE II.   Experimental and fit values of $\Gamma(K^{*0} \to K^0 \gamma)$, $\Gamma(K^{*+} \to K^+ \gamma)$ and $\frac{\Gamma_{K^{*0} \to K^0 \gamma}}{\Gamma_{K^{*+} \to K^+ \gamma}}$.

|  | Experimental | Fit I | Fit II |
|---|---|---|---|
| $\Gamma_{K^{*0} \to K^0 \gamma}$ ($\times 10^{-5}$ GeV) | $11.6 \pm 1.2$ | $13.1 \pm 1.3$ | $14.1 \pm 1.2$ |
| $\Gamma_{K^{*+} \to K^+ \gamma}$ ($\times 10^{-5}$ GeV) | $5.0 \pm 0.6$ | $5.0 \pm 1.0$ | $5.3 \pm 1.0$ |
| $\frac{\Gamma_{K^{*0} \to K^0 \gamma}}{\Gamma_{K^{*+} \to K^+ \gamma}}$ | $2.6 \pm 0.3$ | $2.6 \pm 0.4$ | $2.7 \pm 0.5$ |

results in Table I. Later we will analyze the $\omega \to \pi \gamma^*$ form factor in detail.

Second, regarding the $c_i$ and $d_i$ parameters given in Table I, we see that the resulting values from the two fits are more or less compatible. The situation for the masses and widths of broad resonances is different. Roughly speaking, we observe that the determinations of the masses and widths for $\phi'$ from the two fits are consistent, or at least not so different from each other. This conclusion also holds roughly for the masses of $K^{*'}$. Nevertheless, we find that the masses and widths of $\rho'$ from the two fits are clearly not compatible, indicating that the mass and width of the $\rho'$ are more sensitive to the forms of energy-dependent widths, compared to the $\phi'$ case.

Focusing on the mass and width of $\phi'$, our determinations in Table I are in good agreement with the corresponding parameters of $\phi(1680)$ reported in PDG [31]. Though the mass of $\phi'$ in Ref. [5] is compatible with PDG, its width is somewhat larger. In addition, the uncertainties in our determination of the mass and width for $\phi'$ are much smaller than those obtained in Ref. [5]. Furthermore, we do not need to add the so-called background terms by hand in our amplitude, while this is not the case in the experimental analyses [5]. All of the terms appearing in our amplitudes are obtained from the symmetry allowed operators illustrated in Sec. II A, where the contact terms and contributions from $\rho(770), \omega(782), \phi(1020),$ and $\omega'(1420)$ are incorporated in a consistent way.

Regarding the $\rho'$ resonance, we should mention that the spectra of the excited $\rho$ resonances are still not clear in PDG [31]. The value of the $\rho'$ mass from the recent determination of the SND Collaboration [4] is around 1490 MeV, which is clearly lower than our determinations in Table I. As mentioned previously, we find that the resulting $\rho'$ masses from our fits vary accordingly by using different forms of energy-dependent widths. In Ref. [4], a constant width is used for the $\rho'$ resonance, which is obviously different from ours. We have explicitly checked that if a constant width for the $\rho'$ is used, our determination for its mass decreases to around 1500 MeV in both fits, which becomes close to the value in Ref. [4]. The masses and widths of $\rho'$ from our fits lie between $\rho(1450)$ and $\rho(1700)$. Notice that there are roughly two peaks in the experimental isovector component of the $\sigma_{K^*K}$ cross sections [see Fig. 3(c)], which may be due to the contributions of $\rho(1450)$ and $\rho(1700)$. However, since the statistics are still very poor, we only include one set of the $\rho'$ resonances in the current fit. This indicates that the $\rho'$ here may be regarded as a combined effect of $\rho(1450)$ and $\rho(1700)$.

Finally, we find that the mixing angles of $\omega' - \phi'$ from the two fits are roughly consistent. The resulting angle is around $20°$, and it is clearly different from the ideal mixing case. This indicates that the $1/N_C$ suppressed operator in Eq. (18) is quite important in the determination of the masses of excited vector resonances since the ideal mixing
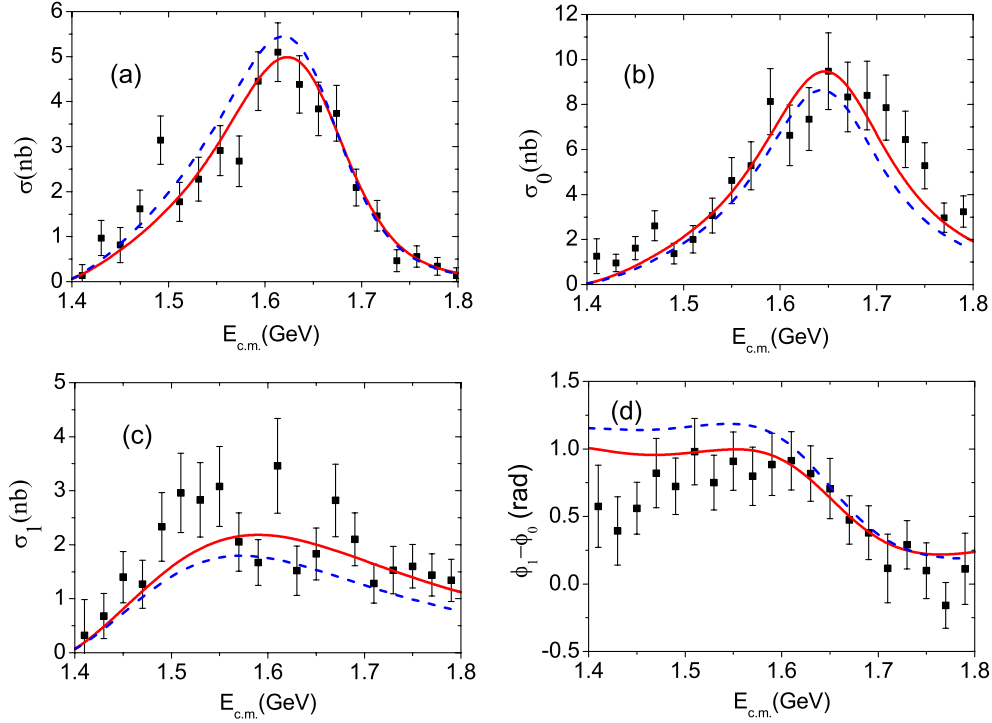
FIG. 3 (color online).   The results of Fit I (red solid line) and Fit II (blue dashed line). Panel (a) displays the cross sections of $\sigma_{K^{*\pm}K^{\mp}}(892)$. Panel (b) displays the isoscalar components of the $\sigma_{K^*K}$. Panel (c) displays isovector components of the $\sigma_{K^*K}$. Panel (d) displays the phase differences between isovector and isoscalar $K^*(892)K$ amplitudes.

will result if only the leading-order operators at large $N_C$ are included for the resonance masses.

## B. Anatomy of the $SU(3)$ breaking mechanism in $K^* \longrightarrow K\gamma$ decays

For the ratio $\frac{\Gamma(K^{*0} \to K^0\gamma)}{\Gamma(K^{*\pm} \to K^\pm\gamma)}$, the $SU(3)$ symmetry tells us that $\frac{\Gamma(K^{*0} \to K^0\gamma)}{\Gamma(K^{*+} \to K^+\gamma)}\big|_{SU(3)} = 4$ [30], while the experimental value is $\frac{\Gamma(K^{*0} \to K^0\gamma)}{\Gamma(K^{*+} \to K^+\gamma)}\big|_{Ex} \simeq 2.3$ [31]. The $SU(3)$ symmetry breaking
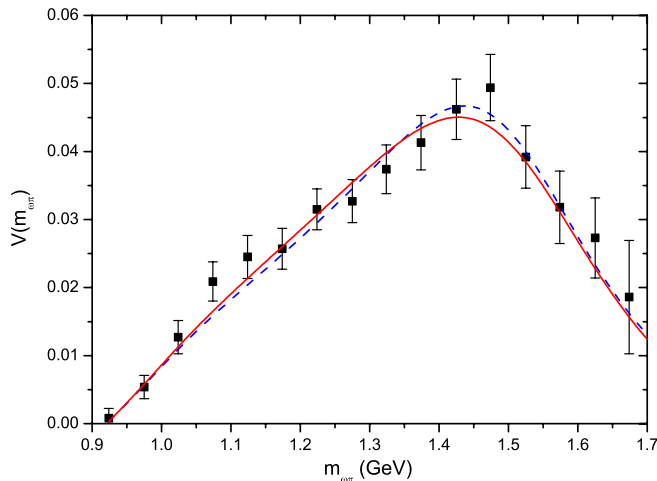


FIG. 4 (color online).   Spectral function for $\tau^- \to \omega\pi^-\nu_\tau$. The experimental data are taken from [45].

effect in the $K^* \longrightarrow K\gamma$ decay has been discussed in many previous works [32–35]. In the context of the VMD model [36], Ref. [32] points out that there is a significant contribution from an intermediate $s\bar{s}$ pair ($\phi$ meson) in these decays, and if all partial $s\bar{s}$ production is suppressed by only (20–30)% relative to those involving nonstrange pairs, the ratio of the neutral to charged $K^*$ decay widths would be brought into line with the data. Including the $SU(3)$ symmetry breaking in the hidden local symmetry model [34,35], it is found that the rate of $\Gamma(K^{*0} \to K^0\gamma)$ is reduced compared to the $SU(3)$ symmetry prediction; in particular, it is pointed out that the vector mesons should be "renormalized" [35].

In the framework of R$\chi$T, there is a special operator in Eq. (13), namely, the $O^4_{\rm VJP}(= \frac{ic_4}{M_V}\epsilon_{\mu\nu\rho\sigma}\langle V^{\mu\nu}[f^{\rho\sigma}_-,\chi_+]\rangle)$ term, which breaks the $SU(3)$ symmetry by the factor $(m_s - m_u)$ and exclusively contributes to the charged processes $K^{*\pm} \to K^\pm\gamma$. Hence, the value of the coupling $c_4$ is important to decode the $SU(3)$ symmetry mechanism in the present work.

In fact, the $c_4$ value has been determined in Ref. [16]. In that reference, the authors only included the lightest multiplet of vector resonances, so the heavier degrees of freedom, such as the excited $\rho'$ state, are implicitly included in their $c_4$. By fitting the first six data points of the isovector component of $e^+e^- \longrightarrow K^*(892)K \to K_S K^\pm\pi^\mp$, they get $c_4 = -0.047 \pm 0.002$, and by fitting the branching ratios of $\tau \longrightarrow K\bar{K}\pi\nu_\tau$, they obtain $c_4 = -0.07 \pm 0.01$. Clearly,
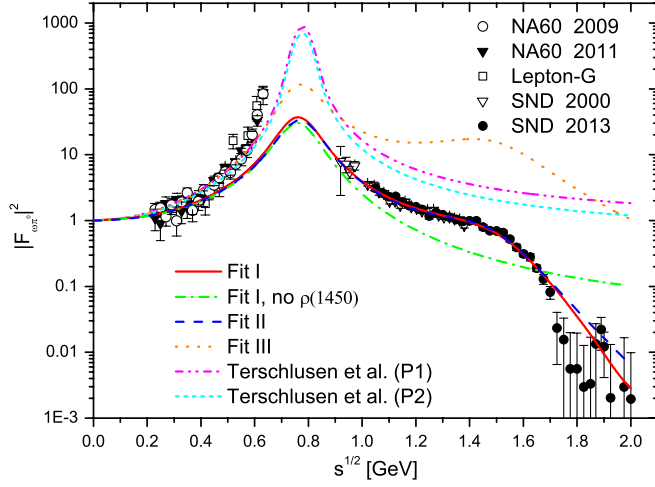
FIG. 5 (color online).   The form factors of $\omega\pi^0\gamma^*$: the data in the left side of 0.8 GeV correspond to the $\omega$-decay processes, and those in the right side correspond to the $\omega$-production processes. The red solid line denotes the result from Fit I, and the blue dashed line denotes the result from Fit II. The green dash-dotted line denotes the prediction of Fit I by simply excluding the contributions from the excited $\rho'$ resonance. The orange dotted line corresponds to the results of Fit III in which the $\omega\pi$ form-factor data from the SND Collaboration and the $\omega\pi$ spectral function data from tau decays are not included in the analysis. The magenta dash-dot-dotted and cyan short-dashed lines correspond to the predictions of the parameter set 1 (P1) and parameter set 2 (P2) in Ref. [48]. Sources of the different experimental data are as follows: open circles [1], solid triangles [2], open squares [44], open triangles [3], and solid circles [4].

neither value determined in Ref. [16] is compatible with our results in Table I, and the magnitudes of $c_4$ in our fits are around 1 order smaller than those in Ref. [16].

We would like to mention that in Ref. [20], an unexpected phenomenon is observed by using $c_4 = -0.07$ in the radiative decay of $\tau \to K\gamma\nu_\tau$. Typically, one would expect that for a low energy cutoff of the photon in $\tau \to K\gamma\nu_\tau$, the decay rate should be dominated by the internal bremsstrahlung (IB) contribution. For example, to take the cutoff for the photon energy at 50 MeV, the IB part contributes more than 90% of the decay rate for the $\tau \to \pi\gamma\nu_\tau$ process (see Table I in Ref. [20]). However, if one looks at Table II in the same reference, the contribution from the IB part in $\tau \to K\gamma\nu_\tau$ dramatically decreases to 6% by taking $c_4 = -0.07$, and in this case, the $c_4$ term dominates the whole process. In the case with $c_4 = 0$, one can see some reasonable results. This clearly gives us a hint that the large magnitude of $c_4$ (compared to 0.07) does not lead to reasonable results in the radiative tau decays. Therefore, our current determination for $c_4$, around 1 order smaller in magnitude than the values given in Ref. [16], seems more meaningful. However, due to the lack of experimental measurements on the radiative tau decays, we still cannot make a concrete conclusion as to whether the $c_4$ values in Table I will reasonably describe the $\tau \to K\gamma\nu_\tau$ process.

A future measurement on this channel is definitely helpful to answer this question.

In order to have a better understanding of the origin of the differences for the $c_4$ values between ours and Ref. [16], we next employ the same VVP Lagrangian as used in Ref. [16], indicating in the discussions below that we exclude the excited vector resonances in our theory. In this case, it is interesting to point out that after taking into account the high energy constraints given in the previous work [14,21],

$$4c_3 + c_1 = 0,$$

$$c_1 - c_2 + c_5 = 0,$$

$$c_5 - c_6 = \frac{N_C}{64\pi^2}\frac{M_V}{\sqrt{2}F_V},$$

$$d_1 + 8d_2 - d_3 = \frac{F^2}{8F_V^2},$$

$$d_3 = -\frac{N_C}{64\pi^2}\frac{M_V^2}{F_V^2}, \tag{43}$$

we can totally predict the $K^{*0} \to K^0\gamma$ decay width, which turns out to be 109.1 KeV and agrees well with the experimental value $(116.2 \pm 11.6)$ KeV [31]. For the charged process $K^{*+} \to K^+\gamma$, we only have one free parameter, $c_4$, to determine its decay width. Therefore, one could use the experimental information $\Gamma_{K^{*+} \to K^+\gamma} = (50.3 \pm 5.5)$ KeV to determine the value of $c_4$. We then obtain two solutions,

$$c_4 = 0.0003 \pm 0.0007 \quad \text{or} \quad -0.0251 \pm 0.0007. \tag{44}$$

By setting $c_4 = -0.0251 \pm 0.0007$ in the decay amplitudes, we find that the $c_4$ term then dominates the $K^{*+} \to K^+\gamma$ process, which indicates that the $SU(3)$ symmetry breaking effect overwhelmingly controls this process and clearly contradicts a general rule that this effect should be at most around 30%. This tells us that only the solution of $c_4 = 0.0003 \pm 0.0007$ in Eq. (44) corresponds to the physical one. Indeed, this observation also confirms the conclusion about the role of $c_4$ in radiative tau decays [20], where a small magnitude of $c_4$ is preferred. In the determination of Eq. (44), we do not explicitly include the vector resonance excitations, and the corresponding results after the incorporation of the excited states can be found in Table I, where the magnitude of $c_4$ is still 1 order smaller than that in Ref. [16]. In the present work, we provide another important and easy way to determine the $c_4$ value, comparing with Ref. [16], which can be useful for the future study of various tau decays.

In order to have a clear idea about how different parts contribute to the $SU(3)$ breaking, we decompose the amplitudes $g_{K^{*0}K^0\gamma}$ and $g_{K^{*+}K^+\gamma}$ in Eqs. (30) and (31) into two parts: the $SU(3)$ symmetric term and the $SU(3)$ breaking term. The decomposition takes the form

$$
\begin{aligned}
g_{K^{*0}K^0\gamma}^{SU(3)\text{symmetry}} = &-\frac{4\sqrt{2}}{3F_K M_V M_{K^*}}[(c_1 + c_2 + 8c_3 - c_5)m_K^2 + (c_2 + c_5 - c_1 - 2c_6)M_{K^*}^2] \\
&- \frac{2F_V}{3F_K M_{K^*}}\left(\frac{1}{M_V^2} - \frac{3}{M_V^2} - \frac{2}{M_V^2}\right)[(d_1 + 8d_2 - d_3)m_K^2 + d_3 M_{K^*}^2] \\
&- \frac{F_{V_1}}{3F_K M_{K^*}}\left(\frac{1}{M_{V_1}^2} - \frac{3}{M_{V_1}^2} - \frac{2}{M_{V_1}^2}\right)(d_m m_K^2 + d_M M_{K^*}^2), \\
g_{K^{*0}K^0\gamma}^{SU(3)\text{breaking}} = &-\frac{2F_V}{3F_K M_{K^*}}\left[\left(\frac{1}{M_\omega^2} - \frac{3}{M_\rho^2} - \frac{2}{M_\phi^2}\right)\right. \\
&\left.- \left(\frac{1}{M_V^2} - \frac{3}{M_V^2} - \frac{2}{M_V^2}\right)\right][(d_1 + 8d_2 - d_3)m_K^2 + d_3 M_{K^*}^2] \\
&- \frac{F_{V_1}}{3F_K M_{K^*}}\left\{\left[\frac{(2\sqrt{2}\cos\theta_V - \sin\theta_V)\sin\theta_V}{M_{\omega'}^2} - \frac{3}{M_{\rho'}^2} - \frac{(\cos\theta_V + 2\sqrt{2}\sin\theta_V)\cos\theta_V}{M_{\phi'}^2}\right]\right. \\
&\left.- \left(\frac{1}{M_{V_1}^2} - \frac{3}{M_{V_1}^2} - \frac{2}{M_{V_1}^2}\right)\right\}(d_m m_K^2 + d_M M_{K^*}^2),
\end{aligned}
\tag{45}
$$

$$
\begin{aligned}
g_{K^{*+}K^+\gamma}^{SU(3)\text{symmetry}} = &\frac{2\sqrt{2}}{3F_K M_V M_{K^*}}[(c_1 + c_2 + 8c_3 - c_5)m_K^2 + (c_2 + c_5 - c_1 - 2c_6)M_{K^*}^2] \\
&- \frac{2F_V}{3F_K M_{K^*}}\left(\frac{1}{M_V^2} + \frac{3}{M_V^2} - \frac{2}{M_V^2}\right)[(d_1 + 8d_2 - d_3)m_K^2 + d_3 M_{K^*}^2] \\
&- \frac{F_{V_1}}{3F_K M_{K^*}}\left(\frac{1}{M_{V_1}^2} + \frac{3}{M_{V_1}^2} - \frac{2}{M_{V_1}^2}\right)(d_m m_K^2 + d_M M_{K^*}^2), \\
g_{K^{*+}K^+\gamma}^{SU(3)\text{breaking}} = &-\frac{2F_V}{3F_K M_{K^*}}\left[\left(\frac{1}{M_\omega^2} + \frac{3}{M_\rho^2} - \frac{2}{M_\phi^2}\right)\right. \\
&\left.- \left(\frac{1}{M_V^2} + \frac{3}{M_V^2} - \frac{2}{M_V^2}\right)\right][(d_1 + 8d_2 - d_3)m_K^2 + d_3 M_{K^*}^2] \\
&- \frac{F_{V_1}}{3F_K M_{K^*}}\left\{\left[\frac{(2\sqrt{2}\cos\theta_V - \sin\theta_V)\sin\theta_V}{M_{\omega'}^2} + \frac{3}{M_{\rho'}^2} - \frac{(\cos\theta_V + 2\sqrt{2}\sin\theta_V)\cos\theta_V}{M_{\phi'}^2}\right]\right. \\
&\left.- \left(\frac{1}{M_{V_1}^2} + \frac{3}{M_{V_1}^2} - \frac{2}{M_{V_1}^2}\right)\right\}(d_m m_K^2 + d_M M_{K^*}^2) + \frac{16\sqrt{2}}{3F_K M_V M_{K^*}}c_4(m_K^2 - m_\pi^2).
\end{aligned}
\tag{46}
$$

The criteria to make the above decomposition is that in the $SU(3)$ symmetric terms, we do not distinguish the mass differences of intermediate vectors and we also assume the ideal mixing for $\omega' - \phi'$. So it is easy to check that $|g_{K^{*0}K^0\gamma}^{SU(3)\text{symmetry}}/g_{K^{*+}K^+\gamma}^{SU(3)\text{symmetry}}| = 2$, consistent with the $SU(3)$ symmetry requirement. However, for the $SU(3)$ breaking parts, there are three sources: different masses of the intermediate vector resonances, the nonideal mixing angle of the $\omega' - \phi'$, and the $c_4$ term in the charged process.

The mass differences and the mixing angle of $\omega' - \phi'$ are directly related to the resonance operators in Eqs. (8) and (18). Therefore, it is crucial to include these mass splitting parameters in the Lagrangian approach in order to systematically study the $SU(3)$ symmetry mechanism.

Next, let us take the results from Fit I in Table I to make a concrete analysis on the strengths of different parts contributing to the $SU(3)$ symmetry breaking. The following numbers can be straightforwardly obtained according to the parameters from Fit I in Table I:

$$\frac{g_{K^{*0}K^0\gamma}}{g_{K^{*+}K^+\gamma}} = \frac{\overset{SU(3)\text{symmetry}}{g_{K^{*0}K^0\gamma}} + \overset{SU(3)\text{breaking}}{g_{K^{*0}K^0\gamma}}}{g_{K^{*+}K^+\gamma}^{SU(3)\text{symmetry}} + (g_{K^{*+}K^+\gamma}^{SU(3)\text{breaking}} - g_{K^{*+}K^+\gamma}^{c_4}) + g_{K^{*+}K^+\gamma}^{c_4}} = \frac{-16.1 + 2.5}{8.0 + 2.0 - 1.6}. \tag{47}$$

It is obvious that these $SU(3)$ breaking effects suppress the neutral $K^*$ decay width but enhance the charged $K^*$ mode; as a result, the ratio between them becomes compatible with the data. Notice that among the $SU(3)$ breaking effects in $K^{*+} \to K^+\gamma$, the $c_4$ term contributes at the same order as the other $SU(3)$ breaking effects in R$\chi$T, although the values of the $c_4$ parameter, with the order of $10^{-3}$ in Table I, seem unnaturally small. The small magnitude of $c_4$ can be attributed to the normalization of the VJP operators in Eq. (13). This conclusion can be easily verified by comparing the values of other VJP couplings with $c_4$. We notice that one VJP operator is considered in Ref. [48], namely, the $e_A$ term in Eq. (15) of that reference. It is easy to obtain that the $e_A$ term is related to our $c_6$ term in Eq. (13) through $c_6 = e_A/(8\sqrt{2}e)$, with $e_A$ estimated to be around $1.5 \times 10^{-2}$ in Ref. [48], which leads to $c_6 \simeq 4.4 \times 10^{-3}$. Therefore, we show that the magnitude of the $c_4$ parameter given in Table I is at the same order as other $c_i$ couplings in the VJP Lagrangian (13) estimated from other works.

## C. Discussion on the $\omega \longrightarrow \pi^0\gamma^*$ transition form factor

Recently, the new measurements on the $\omega \to \pi^0\gamma^*$ form factors from the NA60 Collaboration [1,2] have activated several updated theoretical works [48–50]. The main problem is that the conventional VMD approach cannot incorporate these data well, so new ideas are proposed to have a deeper understanding as to why the successful VMD is not working here.

In Refs. [48,49], a new counting scheme, different from R$\chi$T, is used: the masses of both vector mesons and pseudoscalar mesons are treated as small expansion parameters. So in their counting scheme, the Lagrangian that accounts for the decay mechanism through exchanging an intermediate vector meson belongs to the leading order, while the Lagrangian responsible for the contact terms in the decay amplitude belongs to the next-to-leading order. In Ref. [48], all of the leading-order contributions in their scheme and some incomplete parts of next-to-leading-order contributions are considered in their $\omega \to \pi^0\gamma^*$ form factor. After a careful check, we realize that the VVP-type of Lagrangian in Eq. (14) involving the lowest vector multiplet coincides with the so-called leading-order Lagrangian proposed in Ref. [48] up to some normalization factors. For example, from Eqs. (10) and (15) of Ref. [48], it is easy to see that their $b_A$ corresponds to our

$d_2$, and their $h_A$ relates to our $d_1 + d_3$.[1] The $e_A$ term in Ref. [48], which belongs to the next-to-leading order in their counting, is equivalent to our $c_6$ term, one of the six VJP-type operators in Eq. (13). One should notice that the authors in Ref. [48] mostly focus on the leading-order computation, and in order to make a rough quantitative estimate on the next-to-leading-order effects, they select a particular operator to perform the numerical discussion. In our case, the contact terms, i.e., the VJP operators in Eq. (13), are not suppressed by any counting rule and are fully included in the analyses. Also, the excited vector resonances are not considered in Refs. [48,49].

Though we have some similar operators from the beginning, the QCD high energy behavior is not appreciated in the discussion of Refs. [48,49]. As we have mentioned in the Introduction, the transition form factor with a proper high energy constraint can be directly applied to other physical quantities, such as the light-by-light scattering. Thus, we consider it an improvement to impose the QCD short-distance constraints in the form factor.

Next we make a close comparison with Refs. [48,49]. They employ a theoretical framework similar to ours, but different experimental data are analyzed. The focus of Refs. [48,49] is the $\omega \to \pi^0\gamma^*$ form factors from the $\omega$ decay process, not from the $\omega$ production. It turns out that the form factors in Refs. [48,49] can describe the $\omega \to \pi^0\gamma^*$ data from the NA60 Collaboration fairly well. Then, it is interesting for us to perform another fit to only consider the same type of data as in Refs. [48,49], which will be referred to as Fit III. To be more specific, we only include the form-factor data from the $\omega$ decay [1,2,44] in Fit III and exclude these from the $\omega$ production [3,4] and the $\tau^- \to \omega\pi^-\nu_\tau$ spectral function [45]. As shown in Fig. 5, the final output of our Fit III (the orange dotted line) tends to be quite similar to those from Ref. [48] in the focused energy region, which is below the $\omega$ mass. However, we observe that the $\omega\pi$ form factors in the production region are clearly incompatible with the data from the SND Collaboration, taking the resulting parameters from Fit III (see the orange

---

[1]Using the Shouten identity $g_{\sigma\rho}\epsilon_{\alpha\beta\mu\nu} + g_{\sigma\alpha}\epsilon_{\beta\mu\nu\rho} + g_{\sigma\beta}\epsilon_{\mu\nu\rho\alpha} + g_{\sigma\mu}\epsilon_{\nu\rho\alpha\beta} + g_{\sigma\nu}\epsilon_{\rho\alpha\beta\mu} = 0$ and the equation of motion $\nabla^\mu u_\mu = \frac{i}{2}(\chi_- - \frac{1}{N_F}\langle\chi_-\rangle)$ [13], we have $d_1\epsilon_{\mu\nu\rho\sigma}\langle\{V^{\mu\nu}, V^{\rho\alpha}\}\nabla_\alpha u^\sigma\rangle = \frac{1}{4}d_1\epsilon_{\mu\nu\rho\sigma}\langle\{V^{\mu\nu}, V^{\rho\sigma}\}\nabla_\alpha u^\alpha\rangle = \frac{i}{8}d_1\epsilon_{\mu\nu\rho\sigma}\langle\{V^{\mu\nu}, V^{\rho\sigma}\}\chi_-\rangle - \frac{i}{12}d_1\epsilon_{\mu\nu\rho\sigma}\langle V^{\mu\nu}V^{\rho\sigma}\rangle\langle\chi_-\rangle$. The last term with two traces can be neglected, as it is $1/N_C$ suppressed. Since the parameters of $d_1$ and $d_2$ always appear in the combination as $d_1 + 8d_2$ in our case, the number of independent terms with two vector resonances in this work agrees with that used in Ref. [48].

dotted lines in the region above 0.9 GeV in Fig. 5). Similarly, we find that the form factors in Refs. [48,49], when extrapolated to the production region,[2] are in contradiction with the SND data as well (see the magenta dot-dot-dashed and the cyan dashed lines in Fig. 5). This tells us that a good reproduction of the form factors in $\omega$ decay does not necessarily guarantee a consistent description of the form factors in $\omega$ production. Therefore, it is important to consider both types of data simultaneously, as done in our Fit I and Fit II. After including the SND and CLEO data in the analysis, i.e., the fits presented in Table I, we find that our description of the NA60 data becomes obviously worse (see the difference between the red solid line and the orange dotted line in Fig. 5). It turns out that our theoretical framework starts to be incompatible with the NA60 data above 0.5 GeV.

In this work, the excited vectors are explicitly included, which are obviously important in the $\omega$ production processes from the SND [3,4] and CLEO [45] measurements on the $\omega\pi$ form factors. However, it is also interesting to see to what extent the excited vector resonances can affect the $\omega\pi$ form factor in the $\omega$ decay, i.e., the energy region below $M_\omega - m_\pi$. In Fig. 5, we designate the green dot-dashed line to the situation in which we simply exclude the $\rho'$ contribution. It is obvious that the $\rho'$ plays an important role in describing the SND Collaboration data, while its effect in the low energy region is quite small.

To briefly summarize the fit to the $\omega\pi$ form factor, we could describe the NA60 data in our case to the same extent as in Refs. [48,49], if we had not considered the SND and CLEO data. After the inclusion of the latter two measurements, we conclude that our description is still inadequate for the $\omega \to \pi\gamma^*$ form factors from the NA60 measurements in the energy region near the kinematical boundary, i.e., $M_\omega - m_\pi$. Hence, this is still an open problem in our framework.

## IV. CONCLUSIONS

In this work, the resonance chiral theory is used to study $K^*(892) \to K\gamma$, $e^+e^- \to K^*(892)K$ processes, the $\omega\pi^0\gamma^*$

transition form factor, and the spectral function for $\tau^- \to \omega\pi^-\nu_\tau$. By fitting the corresponding experimental data, the values of resonance couplings, which cannot be fixed through the QCD high energy constraints, are then provided. The masses and widths of our $\phi'$ resonance are quite compatible with the $\phi(1680)$ in PDG [31], while our $\rho'$ looks more like a combined effect of the proposed $\rho(1450)$ and $\rho(1700)$ from PDG. The mass and width of the $\rho'$ resonance are found to be sensitive to the forms of the energy-dependent widths used in the propagator, while the parameters for the $\phi'$ are more or less stable. The resulting values of the $\omega' - \phi'$ mixing angle are found to be around $20°$, clearly different from the ideal mixing case as in the $\omega - \phi$ case. The resonance coupling $c_4$ obtained here is around 1 order smaller in magnitude than those in the literature, and our results seem more meaningful when considering the radiative tau decays. With the $c_4$ value obtained here, we analyze the different $SU(3)$ breaking effects contributing to the ratio of $\frac{\Gamma(K^{*0} \to K^0\gamma)}{\Gamma(K^{*\pm} \to K^\pm\gamma)}$ in detail. And we find that the three sources of $SU(3)$ symmetry breaking effects, e.g., the different masses of intermediate resonances, the nonideal mixing angle of $\omega' - \phi'$, and the nonvanishing value of $c_4$, are more or less equally important at the numerical level.

The excited vector resonances are found to be essential to reproduce the $\gamma^* \to \omega\pi^0$ form-factor data from SND and the CLEO $\omega\pi$ spectral function from tau decays. Although the low energy $\omega\pi$ form-factor data from NA60 can be well reproduced in our approach, the steep-rise behavior close to the upper kinematical boundary region, $\sqrt{s} \leq M_\omega - m_\pi$, is still not fully understood in the current work, even after taking into account the excited vector resonances.

---

[2]The plots in the energy region above $M_\omega - m_\pi$ are not explicitly given in Refs. [48,49]. We have exploited the theoretical formulas presented in the references to plot the curves in Fig. 5.

[1] R. Arnaldi *et al.* (NA60 Collaboration), Phys. Lett. B **677**, 260 (2009).

[2] G. Usai (NA60 Collaboration), Nucl. Phys. **A855**, 189 (2011).

[3] M. N. Achasov *et al.* (SND Collaboration), Phys. Lett. B **486**, 29 (2000).

[4] M. N. Achasov *et al.* (SND Collaboration), Phys. Rev. D **88**, 054013 (2013).

[5] B. Aubert *et al.* (*BABAR* Collaboration), Phys. Rev. D **77**, 092002 (2008).

[6] F. Jegerlehner and A. Nyffeler, Phys. Rep. **477**, 1 (2009).

[7] J. Bijnens, E. Pallante, and J. Prades, Nucl. Phys. **B474**, 379 (1996).

[8] J. Bijnens, E. Pallante, and J. Prades, Nucl. Phys. **B626**, 410 (2002).

[9] G. Ecker, J. Gasser, A. Pich, and E. de Rafael, Nucl. Phys. **B321**, 311 (1989).

[10] S. Weinberg, Physica (Amsterdam) **96A**, 327 (1979).

[11] J. Gasser and H. Leutwyler, Ann. Phys. (N.Y.) **158**, 142 (1984); Nucl. Phys. **B250**, 465 (1985).

[12] G. Ecker, J. Gasser, H. Leutwyler, A. Pich, and E. de Rafael, Phys. Lett. B **223**, 425 (1989).

[13] V. Cirigliano, G. Ecker, M. Eidemüller, R. Kaiser, A. Pich, and J. Portolés, Nucl. Phys. **B753**, 139 (2006).

[14] P. D. Ruiz-Femenia, A. Pich, and J. Portoles, J. High Energy Phys. 07 (2003) 003.

[15] M. Jamin, A. Pich, and J. Portoles, Phys. Lett. B **640**, 176 (2006); **664**, 78 (2008).

[16] D. Gomez Dumm, P. Roig, A. Pich, and J. Portoles, Phys. Rev. D **81**, 034031 (2010).

[17] V. Mateu and J. Portoles, Eur. Phys. J. C **52**, 325 (2007).

[18] Z. H. Guo, J. J. Sanz Cillero, and H. Q. Zheng, J. High Energy Phys. 06 (2007) 030.

[19] Z. H. Guo, Phys. Rev. D **78**, 033004 (2008).

[20] Z.-H. Guo and P. Roig, Phys. Rev. D **82**, 113016 (2010).

[21] Y. H. Chen, Z. H. Guo, and H. Q. Zheng, Phys. Rev. D **85**, 054018 (2012).

[22] P. Roig and J. J. Sanz-Cillero, Phys. Lett. B **733**, 158 (2014).

[23] M. Knecht and A. Nyffeler, Eur. Phys. J. C **21**, 659 (2001).

[24] K. Kampf and J. Novotny, Phys. Rev. D **84**, 014036 (2011).

[25] S. Peris, M. Perrottet, and E. de Rafael, J. High Energy Phys. 05 (1998) 011; M. Knecht, S. Peris, M. Perrottet, and E. de Rafael, Phys. Rev. Lett. **83**, 5230 (1999); S. Peris, B. Phily, and E. de Rafael, Phys. Rev. Lett. **86**, 14 (2001); P. Masjuan and S. Peris, J. High Energy Phys. 05 (2007) 040.

[26] R. Escribano, S. Gonzalez-Solis, and P. Roig, J. High Energy Phys. 10 (2013) 039.

[27] J. A. Oller, E. Oset, and J. E. Palomar, Phys. Rev. D **63**, 114009 (2001).

[28] R. Escribano, P. Masjuan, and J. J. Sanz-Cillero, J. High Energy Phys. 05 (2011) 094.

[29] Z.-H. Guo and J. A. Oller, Phys. Rev. D **84**, 034005 (2011); Z. -H. Guo, J. A. Oller, and J. Ruiz de Elvira, Phys. Rev. D **86**, 054006 (2012).

[30] P. J. O'Donnell, Rev. Mod. Phys. **53**, 673 (1981).

[31] J. Beringer *et al.*, Phys. Rev. D **86**, 010001 (2012).

[32] J. W. Durso, Phys. Lett. B **184**, 348 (1987).

[33] E. Bagan, A. Bramon, and F. Cornet, Phys. Rev. D **31**, 2270 (1985).

[34] A. Bramon, A. Grau, and G. Pancheri, Phys. Lett. B **344**, 240 (1995).

[35] M. Benayouna, L. DelBuonoa, S. Eidelmana, V. N. Ivanchenkoa, and H. B. O. Connell, Phys. Rev. D **59**, 114027 (1999).

[36] J. J. Sakurai, Ann. Phys. (N.Y.) **11**, 1 (1960); J.J. Sakurai, *Currents and Mesons* (University of Chicago Press, Chicago, 1969).

[37] F. Klingl, N. Kaiser, and W. Weise, Z. Phys. A **356**, 193 (1996).

[38] R. I. Dzhelyadin *et al.*, Phys. Lett. **102B**, 296 (1981).

[39] A. Faessler, C. Fuchs, and M. I. Krivoruchenko, Phys. Rev. C **61**, 035206 (2000).

[40] V. Cirigliano, G. Ecker, H. Neufeld, and A. Pich, J. High Energy Phys. 06 (2003) 012.

[41] Zhi-Hui Guo and J. J. Sanz-Cillero, Phys. Rev. D **79**, 096006 (2009).

[42] Z.-H. Guo and J. J. Sanz-Cillero, Phys. Rev. D **89**, 094024 (2014).

[43] W. J. Marciano and A. Sirlin, Phys. Rev. Lett. **61**, 1815 (1988).

[44] R. I. Dzhelyadin *et al.*, Phys. Lett. **102B**, 296 (1981); JETP Lett. **33**, 228 (1981).

[45] K. W. Edwards *et al.* (CLEO Collaboration), Phys. Rev. D **61**, 072003 (2000).

[46] D. Gomez Dumm, A. Pich, and J. Portoles, Phys. Rev. D **62**, 054014 (2000).

[47] E. Arganda, M. J. Herrero, and J. Portoles, J. High Energy Phys. 06 (2008) 079.

[48] C. Terschlüsen and S. Leupold, Phys. Lett. B **691**, 191 (2010).

[49] C. Terschlüsen, S. Leupold, and M. F. M. Lutz, arXiv:1204.4125.

[50] S. P. Schneider, B. Kubis, and F. Niecknig, Phys. Rev. D **86**, 054013 (2012).